

## The Role of Conserved Arginine Residue in Loop 4 of Glycoside Hydrolase Family 10 Xylanases

Mamoru NISHIMOTO,<sup>1</sup> Motomitsu KITAOKA,<sup>1,†</sup> Shinya FUSHINOBU,<sup>2</sup> and Kiyoshi HAYASHI<sup>1</sup>

<sup>1</sup>National Food Research Institute, 2-1-12 Kannondai, Tsukuba, Ibaraki 305-8642, Japan

<sup>2</sup>Department of Biotechnology, The University of Tokyo, 1-1-1 Yayoi, Bunkyo-ku, Tokyo 113-8657, Japan

Received October 4, 2004; Accepted February 10, 2005

**An arginine residue in loop 4 connecting  $\beta$  strand 4 and  $\alpha$ -helix 4 is conserved in glycoside hydrolase family 10 (GH10) xylanases. The arginine residues, Arg<sup>204</sup> in xylanase A from *Bacillus halodurans* C-125 (XynA) and Arg<sup>196</sup> in xylanase B from *Clostridium stercoararium* F9 (XynB), were replaced by glutamic acid, lysine, or glutamine residues (XynA R204E, K and Q, and XynB R196E, K and Q). The pH- $k_{\text{cat}}/K_m$  and the pH- $k_{\text{cat}}$  relationships of these mutant enzymes were measured. The  $pK_{\text{e}2}$  and  $pK_{\text{e}2}$  values calculated from these curves were 8.59 and 8.29 (R204E), 8.59 and 8.10 (R204K), 8.61 and 8.19 (R204Q), 7.42 and 7.19 (R196E), 7.49 and 7.18 (R196K), and 7.86 and 7.38 (R196Q) respectively. Only the  $pK_{\text{e}2}$  value of arginine derivatives was less than those of the wild types (8.49 and 9.39 [XynA] and 7.62 and 7.82 [XynB]). These results suggest that the conserved arginine residue in GH10 xylanases increases the  $pK_a$  value of the proton donor Glu during substrate binding. The arginine residue is considered to clamp the proton donor and subsite +1 to prevent structural change during substrate binding.**

**Key words:** glycoside hydrolase family 10 (GH10); xylanase; pH activity; arginine

Xylanase (EC3.2.1.8) catalyzes the hydrolysis of the main polysaccharide chain ( $\beta$ -1,4 xylosyl bond) in xylan, the most abundant component of plant cell walls except for cellulose. Recently, xylanase has been found to be applicable in the paper industry, replacing the use of toxic chlorinated species to remove lignin from kraft pulp.<sup>1,2</sup> Most xylanases are classified into two families based on their amino acid sequence similarity,<sup>3</sup> glycoside hydrolase families 10 and 11 (GH10 and GH11). GH10 xylanase takes a TIM barrel structure.<sup>4–8</sup> Catalytic amino acid residues has been identified as two glutamic acid residues.<sup>9,10</sup> It is known that several amino acid residues are widely conserved as well the catalytic amino acid residues, forming subsite –2 to +1 in GH10 xylanases.<sup>11–13</sup> The roles of some of the amino

acid residues around the active cleft have been determined by mutation analysis and structural analysis with substrate complex.<sup>14–18</sup> We noticed that an arginine residue is conserved near the proton donor glutamic acid residue in the middle of loop 4 following  $\beta$  strand 4 in the three-dimensional structures of GH10 xylanases. Because the arginine residue is located approximately 4 Å from the glutamic acid residue and tyrosine or phenylalanine residues forming a part of subsite +1, the arginine residue does not directly interact with the proton donor glutamic acid residue or substrate binding sites. In this study, we investigated the role of the arginine residue using two GH10 xylanases, xylanase A from *Bacillus halodurans* C-125 (XynA) and xylanase B from *Clostridium stercoararium* F9 (XynB).<sup>19,20</sup> We concluded that the arginine residue plays a role in keeping the  $pK_a$  of the proton donor glutamic acid residue high when the enzyme is bound with a substrate.

### Materials and Methods

*Construction of arginine mutants.* Arginine residues of XynA and XynB were replaced by glutamic acid, lysine, or glutamine residues using mega-primer polymerase chain reaction<sup>21</sup> with KOD plus polymerase (Toyobo, Osaka, Japan), and the primers shown in Table 1. Plasmid DNA of XynA and XynB prepared previously<sup>19</sup> were used as templates. The amplified fragments and pET28a vector (Novagen, Darmstadt, Germany) were digested with *Nco*I and *Xho*I before the ligation step, which employed a DNA ligation kit, Ligation High (Toyobo). In the construction of the expression plasmids, Ile<sup>2</sup> from XynA and Asn<sup>2</sup> from XynB were replaced by Val and Asp respectively, to produce an additional *Nco*I restriction enzyme site. At the C-terminus of each fragment, a Leu-Glu-His-His-His-His sequence was added to facilitate the purification process. The expression plasmids were used to transform *Escherichia coli* BL21 (DE3).

<sup>†</sup> To whom correspondence should be addressed. Tel: +81-29-838-8071; Fax: +81-29-838-7321; E-mail: mkitaoka@nfri.affrc.go.jp

Abbreviations: GH10, glycoside hydrolase family 10; XynA, xylanase A from *Bacillus halodurans* C-125; XynB, xylanase B from *Clostridium stercoararium* F9; pNP-X<sub>2</sub>, *p*-nitrophenyl- $\beta$ -D-xylobioside

**Table 1.** Nucleotide Sequences of the Primers Used for Mega-Primer PCR

	Nucleotide sequence (5' → 3')
XynA-N	<u>CCATGGTT</u> TACACTTTTTAGAAAAGCCTT
XynA-C	<u>CTCGAGAT</u> CAATAAATCTCCAGTAAGCAGG
R204E	AATGTAGTCGGTACCTGTTATTTGATACCATTCGGATTCCT <b>C</b> CAGGCCGCCGCCATCGTC
R204K	AATGTAGTCGGTACCTGTTATTTGATACCATTCGGATTCCT <b>T</b> CAGGCCGCCGCCATCGTC
R204Q	AATGTAGTCGGTACCTGTTATTTGATACCATTCGGATTCCT <b>G</b> CAGGCCGCCGCCATCGTC
XynB-N	<u>TACCATGGATA</u> AAATCTTAAACAAAAAATGGAGCTTAATTTTAACTATGG
XynB-C	<u>ATCCTCGAGT</u> TCCCGCAACCGTGAA
R196E	TACTCGGTACCGGTAATCTGATACCAAGGACTGTTTT <b>C</b> CATACCGCCGG
R196K	TACTCGGTACCGGTAATCTGATACCAAGGACTGTTTT <b>T</b> CATACCGCCGG
R196Q	TACTCGGTACCGGTAATCTGATACCAAGGACTGTTTT <b>G</b> CATACCGCCGG

The restriction enzyme sites are underlined and mutations are indicated by bold letters.

*Production and purification of the recombinant xylanases.* Each transformant was cultivated at 30 °C with shaking in LB medium containing 50 µg/ml kanamycin until the absorbance at 600 nm reached a level of 0.5. Protein expression was then induced by the addition of isopropyl-1-thio-β-D-galactoside at a final concentration of 0.5 mM, followed by further incubation for 20 h at 30 °C with shaking. Mutant enzymes were purified from the cell-free extract prepared from the 100 ml culture described below. The cells were harvested by centrifugation at 15,000 × g for 10 min and then were resuspended in 20 mM sodium phosphate buffer (pH 7.0). The resuspended cells were sonicated using a sonifier (Branson Ultrasonic Corporation, Danbury, CT, U.S.A.), and the cell debris was removed by centrifugation at 17,000 × g for 30 min. Each enzyme was purified using an ÄKTA purifier (Pharmacia Biotech, Uppsala, Sweden) with Ni-NTA agarose (Qiagen, Hilden, Germany) and DEAE-Toyopearl (Tosoh, Tokyo) column chromatography, as described previously.<sup>19)</sup> The homogeneity of the purified enzymes was confirmed by SDS-PAGE analysis.<sup>22)</sup>

*Protein measurement and xylanase activity.* Protein concentrations were determined using theoretical extinction coefficients calculated from the amino acid sequences of the proteins.<sup>23)</sup> The  $E_{1\text{cm}}^{1\%}$ ,<sub>280nm</sub> values calculated for the arginine mutants from XynA and XynB were 20.96 and 17.42 respectively. Xylanase activity was determined by measuring the amount of *p*-nitrophenol liberated from *p*-nitrophenyl-β-D-xylobioside (*p*NP-X<sub>2</sub>)<sup>24)</sup> as substrate. Reactions were performed at 40 °C in 50 mM MES buffer (pH 6.6) containing 0.01% Triton X-100 and 1.3 mM *p*NP-X<sub>2</sub>. The reactions were stopped by the addition of an equal volume of 1 M sodium carbonate solution, and the amount of *p*-nitrophenol generated was quantified by measuring absorbance at 400 nm. One unit of xylanase activity was defined as the amount of the enzyme liberating 1 µmol of *p*-nitrophenol per min under the conditions described above. Xylanase activity for soluble birch wood xylan was measured using the copper–biconchonic acid method.<sup>25)</sup> The soluble xylan was prepared as described

previously.<sup>26)</sup> The enzyme in 25 µl of 20 mM phosphate buffer (pH 7.0) containing 0.04% Triton X-100 was preincubated with 50 µl of various 0.2 M buffer solutions, as described below, for 3 min, and incubated with 25 µl of 0.003% substrate for 5 min. The reaction was stopped by adding 100 µl of copper–biconchonic acid reagent. The reaction mixture was incubated at 100 °C for 15 min and kept on ice for 20 min. Reducing power was measured based on absorbance at 560 nm using xylose as the standard.

*pH-Activity studies of the xylanases.* To investigate the relationships between pH and enzyme activity, each enzyme solution was diluted in 0.13 mM of each of the following buffers, containing 0.01% Triton X-100 with various concentrations of the substrate (0.038–1.14 mM) at the pH levels indicated: citrate (pH 3.2 and 3.7), acetate (pH 3.9, 4.3, 4.8, 5.3, and 5.8), MES (pH 5.2, 5.6, 6.1, and 6.6), HEPES (pH 6.5, 6.9, 7.3, 7.8, and 8.3), and CHES buffer (pH 7.7, 8.2, 8.8, 9.2, and 9.7). The kinetic parameters and  $pK_{es}$  and  $pK_e$  values were calculated by curve-fitting the experimental data to the Michaelis–Menten equation (Eq. 1) and the bell-shaped curves (Eq. 2 and Eq. 3)<sup>27)</sup> using the GraFit computer program.<sup>28)</sup>

$$v = (k_{\text{cat}}[E]_0[S]_0)/(K_m + [S]_0) \quad (\text{Eq. 1})$$

$$V_{\text{max}}(\text{pH}) = V_{\text{max}}/((10^{(pK_{es1}-\text{pH})} + 1)(10^{(\text{pH}-pK_{es2})} + 1)),$$

( $pK_{es1}$ ,  $pK_a$  for the nucleophile with substrate;  $pK_{es2}$ ,  $pK_a$  for the proton donor with substrate binding)

(Eq. 2)

$$V_{\text{max}}/K_m(\text{pH}) = (V_{\text{max}}/K_m)/((10^{(pK_{e1}-\text{pH})} + 1)(10^{(\text{pH}-pK_{e2})} + 1)),$$

( $pK_{e1}$ ,  $pK_a$  for the nucleophile without substrate;  $pK_{e2}$ ,  $pK_a$  for the proton donor without substrate binding)

(Eq. 3)

The dissociation pattern of the proton donor and nucleophile is illustrated in Fig. 1.

## Results and Discussion

### Modeled structure of XynA and XynB

To confirm that the arginine residue was mutated, the predicted three-dimensional structures of XynA and XynB were constructed on the web site program of SWISS-MODEL (<http://www.expasy.org/swissmod/>)<sup>29</sup> based on the three-dimensional structure of GH10 xylanase from *Geobacillus stearothermophilus* T-6 (PDBID: 1HIZ).<sup>30</sup> They showed 75% and 68% amino acid sequence similarity (Fig. 2A) with XynA and XynB respectively, suggesting the reliability of the general structure. The amino acid sequences of XynA and XynB have 51% identity and 73% similarity. The modeled structure of XynA and XynB are shown in Fig. 2B to be comparable with the template structure. The location of the conserved residues such as catalytic and substrate binding residues were topologically identical with the

template. Around the proton donor residues, the structures of loop 4 were different especially in the front part due to their low similarity. That of XynB was more

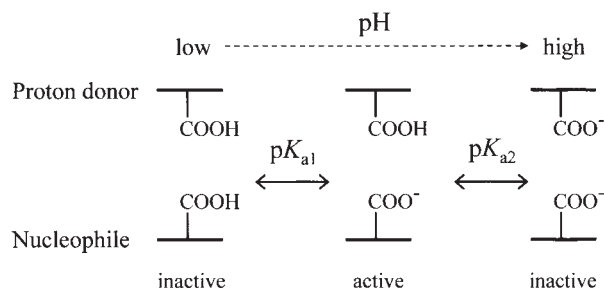


**Fig. 1.** Model for the Dissociation Pattern of an Enzyme Containing Two Catalytic Residues.

$pK_{a1}$  and  $pK_{a2}$  show the dissociation constant for the nucleophile and proton donor residues respectively.

## A

1HIZ	1:MRNVVRKPLTIGLALTLTLLPMTATSANKNAD---S-YAK--KPHISALN--AP-Q-LDQRYKNEFTIGAAVEP-YQLQNEKDVOMLKR	78
XynA	1:MITLFRKPFVAGLAISLIVGGIGNVAAQGGPPKSGVFGENEKRNDQPFQVA-S-LSERYQEQFDIGAAVEP-YQLEGRQA-QILKH	86
XynB	1:-----MNKFLNKKWSLILTMGGIFLMTLSLIFATGKAFNDQTS AEDIPSLAEAFRDYFPIGAAIEPGYTTGQIA--ELYKK	76
	β2..... α2..... β3..... ** α3..... α1.....	
79:	HFNLSVAENVMKPTISIQPEEGKFNFEQADRIVKFAKANGMDIRFHTLVVHSQVPEWFFLDKEGKPMVNETDPVKREONKQLLLKRLETHI	168
87:	HYNLSVAENAMKPBLSLQPREGEWNWEADKIVFARKHNMELRFHTLVVHSQVPEWFFIDEDGNRMVDETDPPKREANKQLLLERMENHI	176
77:	HVNMLVAENAMKPPASLOPTEGNSQWADADRIVQFAKENGMELELRFHTLVVHNTPTGFSLDKEGKPMVEETDPOKREENRKLLELQRLNYI	166
	β4..... * α4..... β5..... * α5.....	
169:	KTIIVERYKDDIKYWDVVNEVYGD--DGKLRNSPWYQIAGIDYIKVAFQAAKYGGDNIKLYMNDYNTVEPKRRTALYNLVKQLEKKEGVPI	256
177:	KTVVERYKDDVTSWVNEVYDD--GGGLRSEWYQITGTDYIKVAFETARKYGGEEAKLYINDYNTVEPSKRDDLYNLVKDLLEQGVPI	264
167:	RAVVLRYKDDIKSWDVVNEVIEPNDPGGMRNSPWYQITGTEYIEVAFRATREAGGSDIKLYINDYNTDDEPKRDLILYELVKNLLEKGVPI	256
	β6..... α6..... β7..... α7..... β8.....	
257:	DGIGHQSHIQIGWPSSEAEFEKTNMF AALGLDNOITELDVS MYGWPPRA-YPTYDAIPKQKFLD-QAARYDRLEKLYEKLSDKISNVTFFW	344
265:	DGVGHQSHIQIGWPSIEDTRASF EKF TSLGLDNOVFE LDM SLYGWPP T GAYTSYDDI PAEL-LQAQADRYDQLFELYEELAADISSVTFW	353
257:	DGVGHQTHIDIYNPVVERTIESIKKFAAGLGLDNIITELDMSIYSWNRSDYG--DSIPDYILTL-QAKRYQELFDALKEKNDIVSAVVFW	343
	α8.....	
345:	GIADNHTWLD SRADVYYDANGNVVDPNAPYAKVEKGGK DAPFVFGPDYKVKPAYWAIIDHK----	407
354:	GIADNHTWLDGRAREYNNVG--I-----DAPFVFDHNYRVKPAYWRIID-----	396
344:	GISDRKYSWLN--G--FP-----VKRTNA-----PLLFDRNFMKPAFWAIVDPSRLRE	387

## B

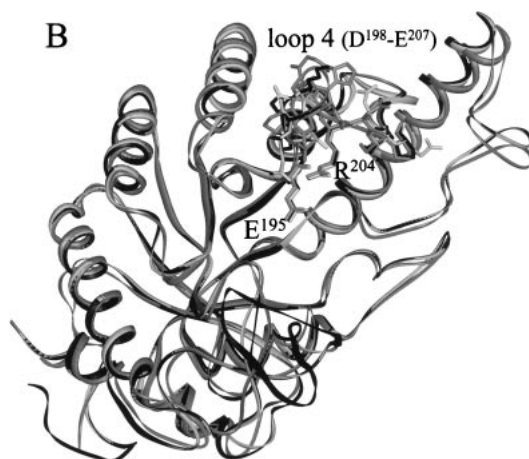


**Fig. 2.** Alignment of Amino Acid Sequences (A) and Modeled Structures (B) for XynA and XynB and Template 1HIZ.

(A) Amino acid sequences of XynA, XynB, and 1HIZ are aligned. Reversal letters represent identical amino acid residues at each position. The region of loop 4 is boxed. Asterisks show the conserved residues in the active center shown in Fig. 4. Dotted lines show  $\alpha$ -helices and  $\beta$ -strands constructing the  $(\beta/\alpha)_8$  barrel. (B) Structures of XynA, XynB, and 1HIZ are shown in ribbon-style, colored white, black, and gray respectively. These structures were superimposed by SWISS Pdb-Viewer software.<sup>29</sup> Amino acid residues, proton donor Glu<sup>195</sup>, and loop 4 constituents containing Arg<sup>204</sup> show a stick form (numbering from XynA).

bulky than those of XynA and 1HIZ because XynB was two amino acid residues longer in the front part of loop 4. But the locations of the arginine residue (Arg<sup>204</sup> for XynA and Arg<sup>196</sup> for XynB) were well conserved, approximately 4.5 Å apart from the side chain of the proton donor residue.

#### Construction of the arginine mutants

To investigate the function of the arginine residue, the strongly basic residues (Arg) in XynA and XynB were replaced by acidic (Glu), neutral (Gln), or less basic (Lys) residues. All the mutated enzymes were expressed as soluble proteins and successfully purified through the His-tag trapping system. They showed hydrolytic activities on both pNP-X<sub>2</sub> and xylan.

#### Basic characterization of the mutant xylanases

The activities of the purified mutant xylanases are listed in Table 2. We report that the  $K_m$  values toward pNP-X<sub>2</sub> of the mutant enzymes were identical with those of the corresponding parental enzyme. The  $k_{cat}$  values on pNP-X<sub>2</sub> of the mutants were slightly less than those of the corresponding parental enzymes, especially with XynA. Specific activities for birch wood xylan also decreased slightly by the mutations, but the differences were not so significant as to establish that the arginine residue was essential in the catalytic action or substrate recognition. Additionally, it should be noted that no significant difference in the activity with the difference in the residues after substitution was observed. Hence we conclude that the arginine residue does not play a direct role in the catalysis of GH10 xylanases.

The thermal stabilities of the parental and mutant xylanases were assessed by determining the residual activity after incubation at 60 °C. The half lives of the activity for mutants were smaller than those of the corresponding parental enzymes, but again the differences were not very significant, only small decreases in a stable temperature range within a few degrees. Thus we do not consider that the stabilization of the enzyme is the main role of the arginine. Furthermore, the decreases in stability did not affect the measurement of pH-activity relationships for mutant enzymes under the assay conditions used.

**Table 2.** Comparison of the Characterization for Arginine Mutants

	$k_{cat}$ for pNP-X <sub>2</sub> (sec <sup>-1</sup> )*	$K_m$ for pNP-X <sub>2</sub> (mM)*	Specific activity for xylan (U/mg) <sup>#</sup>	$t^{1/2}$ at 60 °C (min)*
XynA	32.4	0.20	16.2	59.4
R204E	15.7	0.21	10.2	24.5
R204K	18.9	0.18	12.3	36.6
R204Q	22.5	0.20	12.2	51.7
XynB	58.1	0.09	10.3	249
R196E	50.8	0.14	6.50	101
R196K	51.4	0.10	8.35	123
R196Q	54.3	0.12	8.96	101

The enzyme reaction was performed at pH 6.6 (\*) or pH 7.0 (#).

#### pH-Activity relationships of the mutant xylanases

The pH-activity relationships of the mutant xylanases were measured using pNP-X<sub>2</sub> as a substrate. Relative  $V_{max}/K_m$  and  $V_{max}$  and  $K_m$  values were determined at various pH levels, as shown in Fig. 3. It is obvious that the drastic increases of the parental enzymes in  $K_m$  values with the increase in pH disappeared with the mutation. The  $pK_{es}$  and  $pK_e$  values were calculated by regressing the experimental data with formulae (2) and (3), as shown in Table 3.

Considering the dissociation of the nucleophile glutamic acid residue, small increases in both the  $pK_{e1}$  and  $pK_{es1}$  values were observed with both xylanases, but the  $\Delta_1$  values ( $pK_{es1}-pK_{e1}$ ) did not change with the mutations. The arginine residue might have some weak long-range interaction with the nucleophile.

In the case of the dissociation of the proton donor glutamic acid residue, significant differences in  $pK_{es2}$  were observed, whereas  $pK_{e2}$  did not change with the mutations. The differences are obvious by comparing the difference in  $\Delta_2$  ( $pK_{es2}-pK_{e2}$ ). Both the parental enzymes have positive  $\Delta_2$  values, but those of all the mutants turned negative. These results suggest that the side chain of arginine residue plays an important role in keeping  $pK_{es2}$  value high only when the enzymes form complexes with substrates.

It should be noted that the  $pK_{es2}$  value of all the mutants of each parent were identical even though the charge of the replaced residues were different, indicating that the function of arginine cannot be explained only by the charge of the residue. Thus, the effect of the arginine residues should be related not merely to the charge, but to the whole structure of the arginine.

The location of the amino acid residues well conserved in GH 10 xylanases around Arg<sup>204</sup> in the modeled structure of XynA is schematically illustrated in Fig. 4. The distances between the residues were almost identical with XynB, as shown in Fig. 4. The arginine residue appears not directly to interact with substrate judging from the structure of *G. stearothermophilus* T-6 xylanase with substrate binding (PDB ID: 1R87). The positive charge of Arg<sup>204</sup> appears not directly to interact with the side chain of the proton donor Glu<sup>195</sup> because of the distance of 4.5 Å (between N $\eta$ 2 of Arg<sup>204</sup> and O $\epsilon$ 1 of Glu<sup>195</sup>). This accords with the fact that the  $pK_{e2}$  values did not change with the mutation of the arginine residues.

A charged nitrogen atom of Arg<sup>204</sup> (N $\eta$ 2) was found to make a hydrogen bond with the phenolic oxygen atom of Tyr<sup>239</sup>, which fixed substrates at subsite +1 by stacking interaction.<sup>31)</sup> Roberge *et al.* substituted the conserved tyrosine residue with phenylalanine in *Streptomyces lividans* xylanase A and concluded that this hydrogen bond did not appear to be important for the catalytic activity.<sup>32)</sup> Furthermore, some GH10 xylanases naturally have phenylalanine residue at the position,<sup>12)</sup> again indicating that the phenolic hydroxyl group is not essential for the activity. These results agree with our

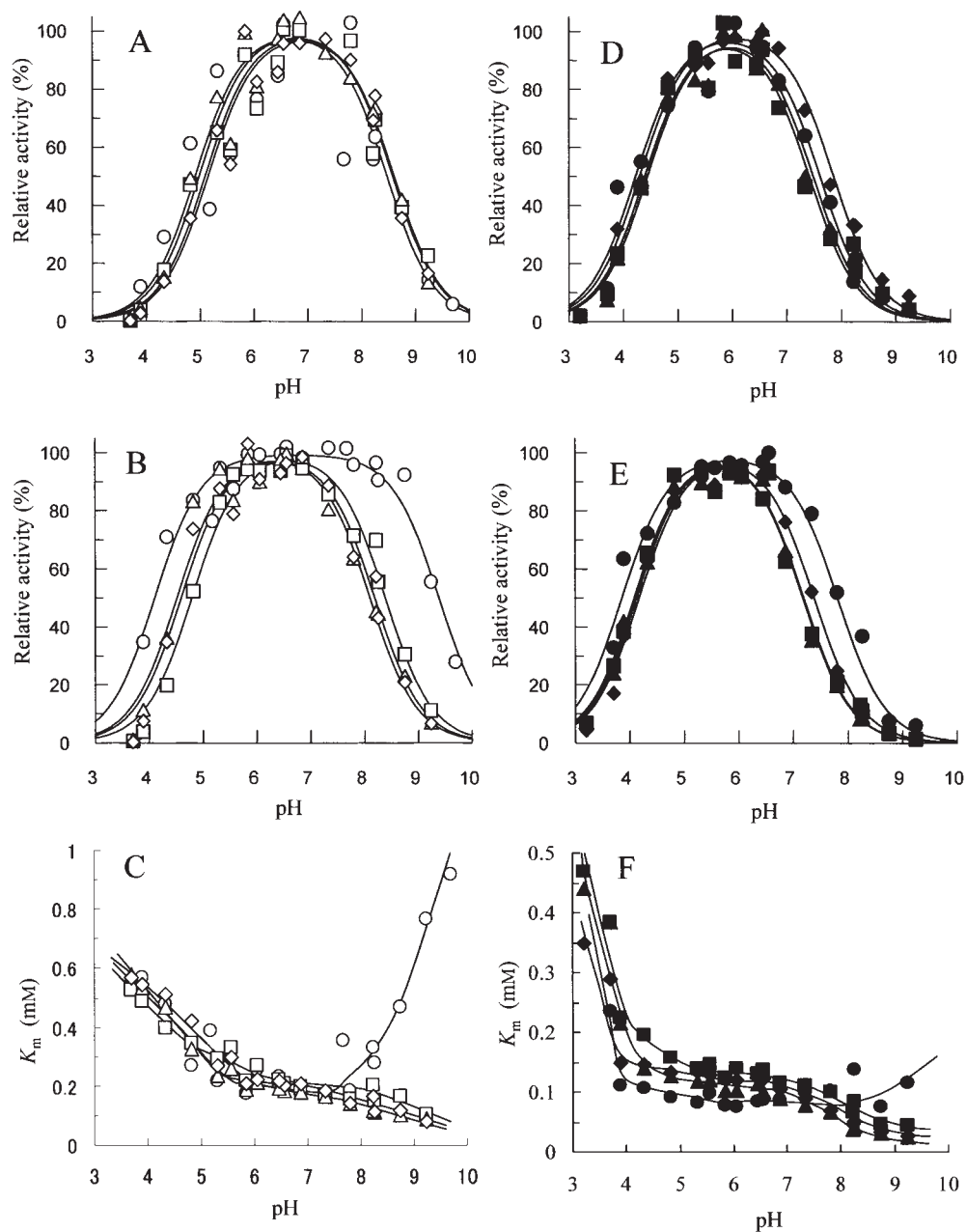


**Fig. 3.** Comparison of pH-Activity Profiles.

These profiles show the pH versus  $V_{\max}/K_m$  (A and D),  $V_{\max}$  (B and E), and  $K_m$  (C and F) for arginine mutants. Open circles, XynA and XynA derivatives; closed circles, XynB and XynB derivatives; circles, wild type; squares, glutamic acid mutants; triangles, lysine mutants; diamonds, glutamine mutants.

**Table 3.** Comparison of  $pK_e$  and  $pK_{es}$  Values for Arginine Mutants

	$pK_{e1}$	$pK_{es1}$	$\Delta_1$	$pK_{e2}$	$pK_{es2}$	$\Delta_2$
XynA						
Wild type	$4.72 \pm 0.21$	$4.10 \pm 0.08$	-0.62	$8.49 \pm 0.18$	$9.39 \pm 0.08$	+0.90
R204E	$5.10 \pm 0.12$	$4.56 \pm 0.07$	-0.56	$8.59 \pm 0.12$	$8.29 \pm 0.06$	-0.30
R204K	$4.99 \pm 0.10$	$4.52 \pm 0.09$	-0.47	$8.59 \pm 0.10$	$8.10 \pm 0.08$	-0.49
R204Q	$5.15 \pm 0.10$	$4.59 \pm 0.09$	-0.56	$8.61 \pm 0.10$	$8.19 \pm 0.08$	-0.42
XynB						
Wild type	$4.23 \pm 0.09$	$3.86 \pm 0.09$	-0.37	$7.62 \pm 0.09$	$7.82 \pm 0.08$	+0.20
R196E	$4.39 \pm 0.09$	$4.09 \pm 0.06$	-0.30	$7.42 \pm 0.09$	$7.19 \pm 0.07$	-0.23
R196K	$4.45 \pm 0.08$	$4.13 \pm 0.06$	-0.32	$7.49 \pm 0.08$	$7.18 \pm 0.08$	-0.31
R196Q	$4.31 \pm 0.07$	$4.18 \pm 0.05$	-0.13	$7.86 \pm 0.06$	$7.38 \pm 0.05$	-0.48

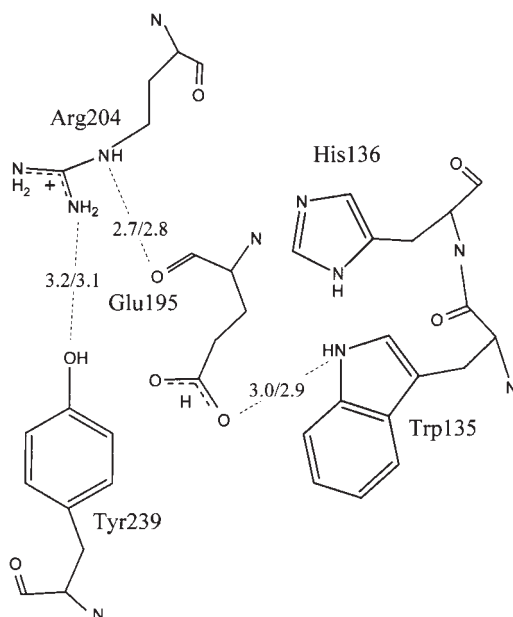


**Fig. 4.** A Schematic Diagram of the Interaction of Well-Conserved Residues in GH 10 Xylanases around Arg<sup>204</sup> in the Modeled Structure of XynA.

Amino acid residues that are the major focus of this paper are represented in line form. The expected hydrogen bond is shown by the dotted line (distances are indicated with XynA/XynB in Å). N $\epsilon$ 2 and N $\epsilon$ 1 atoms of Arg<sup>204</sup> form hydrogen bonds with the phenolic oxygen atom of Tyr<sup>239</sup> and the carbonyl oxygen of the main chain of Glu<sup>195</sup> respectively. Tyr<sup>239</sup> and Trp<sup>135</sup> constitute part of subsite +1 and -1 respectively. N $\epsilon$ 1 of Trp<sup>135</sup> has a hydrogen bond with O $\epsilon$ 1 of Glu<sup>195</sup>. The indole ring of His<sup>136</sup> is located 3.7/3.6, 3.3/3.4, and 3.6/3.4 Å from N $\eta$ 1 of Arg<sup>204</sup>, O $\epsilon$ 1 of Glu<sup>195</sup>, and N $\epsilon$ 1 of Trp<sup>135</sup> respectively.

results that the arginine mutants that lost the hydrogen bond showed comparable activities with the corresponding wild-type enzymes.

The N $\epsilon$  atom of Arg<sup>204</sup> has been found to form a hydrogen bond with the carbonyl oxygen in the main chain of the proton donor Glu<sup>195</sup>. Considering the two hydrogen bonds, Arg<sup>204</sup> might play a role as a structural clamp between proton donor Glu<sup>195</sup> and subsite +1 to protect from structural changes during substrate-binding. This clamping explains the small decreases in thermal stability through the mutations. The clamping might also explain how it is that the effect of the mutation of Arg<sup>204</sup> appeared only with pK<sub>es2</sub>.

The real mechanism in the decrease in pK<sub>es2</sub> is not readily available with the experimental results above, but a possible explanation is the following: His<sup>136</sup> is located close to the proton donor Glu<sup>195</sup> with a distance of 3.3 Å between C $\epsilon$ 1 of His<sup>136</sup> and O $\epsilon$ 1 of Glu<sup>195</sup>. Thus the positive charge of His<sup>136</sup> might affect the pK<sub>a</sub> of the proton donor Glu<sup>195</sup>. The distance between N $\epsilon$ 2 of His<sup>136</sup> and N $\eta$ 1 of Arg<sup>204</sup> is relatively close at 3.7 Å. Arg<sup>204</sup> might prevent His<sup>136</sup> from approaching Glu<sup>195</sup> by preventing a structural change, by clamping the proton donor and subsite +1 or by a steric hindrance. The histidine residue also neighbor Trp<sup>135</sup> and has important

roles for both activity and substrate binding as subsite -1 as demonstrated by mutational analysis.<sup>32,33</sup> Thus the effect of His<sup>136</sup> to Glu<sup>195</sup> might not be direct, but rather through Trp<sup>135</sup>.

In conclusion, the conserved arginine residue plays an important role for GH10 xylanases to keep pK<sub>a</sub> of the proton donor glutamic acid high during substrate binding by clamping the proton donor and subsite +1.

## Acknowledgment

This work was supported in part by a grant from the Bio-oriented Technology Research Advancement Institution.

## References

- 1) Bissoon, S., Christov, L., and Singh, S., Bleach boosting effects of purified xylanase from *Thermomyces lanuginosus* SSBP on bagasse pulp. *Process Biochem.*, **37**, 567–572 (2002).
- 2) La Grange, D. C., Pretorius, I. S., Claeysens, M., and van Zyl, W. H., Degradation of xylan to D-xylose by recombinant *Saccharomyces cerevisiae* coexpressing the *Aspergillus niger*  $\beta$ -xylosidase (xlnD) and the *Trichoderma reesei* xylanase II (xyn2) genes. *Appl. Environ. Microbiol.*, **67**, 5512–5519 (2001).
- 3) Bourne, Y., and Henrissat, B., Glycoside hydrolases and glycosyltransferases: Families and functional modules. *Curr. Opin. Struct. Biol.*, **11**, 593–600 (2001).
- 4) Derewenda, U., Swenson, L., Green, R., Wei, Y., Morosoli, R., Shareck, F., Kluepfel, D., and Derewenda, Z. S., Crystal structure, at 2.6-Å resolution, of the *Streptomyces lividans* xylanase A, a member of the F family of  $\beta$ -1,4-D-glycanases. *J. Biol. Chem.*, **269**, 20811–20814 (1994).
- 5) Fujimoto, Z., Kuno, A., Kaneko, S., Kobayashi, H., Kusakabe, I., and Mizuno, H., Crystal structures of the sugar complexes of *Streptomyces olivaceoviridis* E-86 xylanase: Sugar binding structure of the family 13 carbohydrate binding module. *J. Mol. Biol.*, **316**, 65–78 (2002).
- 6) White, A., Withers, S. G., Gilkes, N. R., and Rose, D. R., Crystal structure of the catalytic domain of the  $\beta$ -1,4-glycanase cex from *Cellulomonas fimi*. *Biochemistry*, **33**, 12546–12552 (1994).
- 7) Harris, G. W., Jenkins, J. A., Connerton, I., Cummings, N., Lo Leggio, L., Scott, M., Hazlewood, G. P., Laurie, J. I., Gilbert, H. J., and Pickersgill, R. W., Structure of the catalytic core of the family F xylanase from *Pseudomonas fluorescens* and identification of the xylpentose-binding sites. *Structure*, **2**, 1107–1116 (1994).
- 8) Natesh, R., Bhanumoorthy, P., Vithayathil, P. J., Sekar, K., Ramakumar, S., and Viswamitra, M. A., Crystal structure at 1.8 Å resolution and proposed amino acid sequence of a thermostable xylanase from *Thermoascus aurantiacus*. *J. Mol. Biol.*, **288**, 999–1012 (1999).
- 9) MacLeod, A. M., Lindhorst, T., Withers, S. G., and Warren, R. A., The acid/base catalyst in the exoglucanase/xylanase from *Cellulomonas fimi* is glutamic acid

- 127: Evidence from detailed kinetic studies of mutants. *Biochemistry*, **33**, 6371–6376 (1994).
- 10) Tull, D., Withers, S. G., Gilkes, N. R., Kilburn, D. G., Warren, R. A., and Abersold, R., Glutamic acid 274 is the nucleophile in the active site of a “retaining” exoglucanase from *Cellulomonas fimi*. *J. Biol. Chem.*, **266**, 15621–15625 (1991).
  - 11) Charnock, S. J., Spurway, T. D., Xie, H., Beylot, M. H., Virden, R., Warren, R. A., Hazlewood, G. P., and Gilbert, H. J., The topology of the substrate binding clefts of glycosyl hydrolase family 10 xylanases are not conserved. *J. Biol. Chem.*, **273**, 32187–32199 (1998).
  - 12) Lo Leggio, L., Jenkins, J., Harris, G. W., and Pickersgill, R. W., X-ray crystallographic study of xylopentaose binding to *Pseudomonas fluorescens* xylanase A. *Proteins*, **41**, 362–373 (2000).
  - 13) Ducros, V., Charnock, S. J., Derewenda, U., Derewenda, Z. S., Dauter, Z., Dupont, C., Shareck, F., Morosoli, R., Kluepfel, D., and Davies, G. J., Substrate specificity in glycoside hydrolase family 10. Structural and kinetic analysis of the *Streptomyces lividans* xylanase 10A. *J. Biol. Chem.*, **275**, 23020–23026 (2000).
  - 14) Andrews, S. R., Charnock, S. J., Lakey, J. H., Davies, G. J., Claeysens, M., Nerinckx, W., Underwood, M., Sinnott, M. L., Warren, R. A., and Gilbert, H. J., Substrate specificity in glycoside hydrolase family 10. Tyrosine 87 and leucine 314 play a pivotal role in discriminating between glucose and xylose binding in the proximal active site of *Pseudomonas cellulosa* xylanase 10A. *J. Biol. Chem.*, **275**, 23027–23033 (2000).
  - 15) Pell, G., Szabo, L., Charnock, S. J., Xie, H., Gloster, T. M., Davies, G. J., and Gilbert, H. J., Structural and biochemical analysis of *Cellvibrio japonicus* xylanase 10C: How variation in substrate-binding cleft influences the catalytic profile of family GH-10 xylanases. *J. Biol. Chem.*, **279**, 11777–11788 (2004).
  - 16) Fujimoto, Z., Kaneko, S., Kuno, A., Kobayashi, H., Kusakabe, I., and Mizuno, H., Crystal structures of decorated xylooligosaccharides bound to a family 10 xylanase from *Streptomyces olivaceoviridis* E-86. *J. Biol. Chem.*, **279**, 9606–9614 (2004).
  - 17) Pell, G., Taylor, E. J., Gloster, T. M., Turkenburg, J. P., Fontes, C. M., Ferreira, L. M., Nagy, T., Clark, S. J., Davies, G. J., and Gilbert, H. J., The mechanisms by which family 10 glycoside hydrolases bind decorated substrates. *J. Biol. Chem.*, **279**, 9597–9605 (2004).
  - 18) Lo Leggio, L., Kalogiannis, S., Eckert, K., Teixeira, S. C. M., Bhat, M. K., Andrei, C., Pickersgill, R. W., and Larsen, S., Substrate specificity and subsite mobility in *T. aurantiacus* xylanase 10A. *FEBS Lett.*, **509**, 303–308 (2001).
  - 19) Nishimoto, M., Kitaoka, M., and Hayashi, K., Employing chimeric xylanases to identify regions of an alkaline xylanase participating in enzyme activity at basic pH. *J. Biosci. Bioeng.*, **94**, 395–400 (2002).
  - 20) Nishimoto, M., Honda, Y., Kitaoka, M., and Hayashi, K., A kinetic study on pH-activity relationship of XynA from alkaliphilic *Bacillus halodurans* C-125 by using aryl-xylobiosides. *J. Biosci. Bioeng.*, **93**, 428–430 (2002).
  - 21) Ke, S. H., and Madison, E. L., Rapid and efficient site-directed mutagenesis by single-tube ‘megaprimer’ PCR method. *Nucleic Acids Res.*, **25**, 3371–3372 (1997).
  - 22) Laemmli, U. K., Cleavage of structural proteins during the assembly of the head of bacteriophage T4. *Nature*, **227**, 680–685 (1970).
  - 23) Gill, S. C., and von Hippel, P. H., Calculation of protein extinction coefficients from amino acid sequence data. *Anal. Biochem.*, **182**, 319–326 (1989).
  - 24) Kitaoka, M., Haga, K., Kashiwagi, Y., Sasaki, T., Taniguchi, H., and Kusakabe, I., Kinetic studies on *p*-nitrophenyl-cellobioside hydrolyzing xylanase from *Cellvibrio gilvus*. *Biosci. Biotechnol. Biochem.*, **57**, 1987–1989 (1993).
  - 25) Waffenschmidt, S., and Jaenicke, L., Assay of reducing sugars in the nanomole range with 2,2′-bichinoninate. *Anal. Biochem.*, **165**, 337–340 (1987).
  - 26) Honda, Y., Kitaoka, M., Sakka, K., Ohmiya, K., and Hayashi, K., An investigation of the pH-activity relationships of Cex, a family 10 xylanase from *Cellulomonas fimi*: Xylan inhibition and the influence of the nitro-substituted aryl- $\beta$ -D-xylobiosides. *J. Biosci. Bioeng.*, **93**, 313–317 (2002).
  - 27) Dixon, M., The effect of pH on the affinities of enzymes for substrates and inhibitors. *Biochem. J.*, **55**, 161–170 (1953).
  - 28) Leatherbarrow, R. J., Using linear and non-linear regression to fit biochemical data. *Trends Biochem. Sci.*, **15**, 455–458 (1990).
  - 29) Guex, N., and Peitsch, M. C., SWISS-MODEL and the Swiss-PdbViewer: An environment for comparative protein modeling. *Electrophoresis*, **18**, 2714–2723 (1997).
  - 30) Teplitsky, A., Mechaly, A., Stojanoff, V., Sainz, G., Golan, G., Feinberg, H., Gilboa, R., Reiland, V., Zolotnitsky, G., Shallom, D., Thompson, A., Shoham, Y., and Shoham, G., Structure determination of the extracellular xylanase from *Geobacillus stearothermophilus* by selenomethionyl MAD phasing. *Acta Crystallogr. D Biol. Crystallogr.*, **60**, 836–848 (2004).
  - 31) Charnock, S. J., Spurway, T. D., Xie, H., Beylot, M. H., Virden, R., Warren, R. A., Hazlewood, G. P., and Gilbert, H. J., The topology of the substrate binding clefts of glycosyl hydrolase family 10 xylanases are not conserved. *J. Biol. Chem.*, **273**, 32187–32199 (1998).
  - 32) Roberge, M., Shareck, F., Morosoli, R., Kluepfel, D., and Dupont, C., Characterization of active-site aromatic residues in xylanase A from *Streptomyces lividans*. *Protein Eng.*, **12**, 251–257 (1999).
  - 33) Charnock, S. J., Lakey, J. H., Virden, R., Hughes, N., Sinnott, M. L., Hazlewood, G. P., Pickersgill, R., and Gilbert, H. J., Key residues in subsite F play a critical role in the activity of *Pseudomonas fluorescens* subspecies *cellulosa* xylanase A against xylooligosaccharides but not against highly polymeric substrates such as xylan. *J. Biol. Chem.*, **272**, 2942–2951 (1997).